Title

Tumor-specific delivery of gemcitabine with activatable liposomes

Authors

Tucci, Samantha T

Kheirolomoom, Azadeh

Ingham, Elizabeth S

et al.

Publication Date

2019-09-01

DOI

10.1016/j.jconrel.2019.07.014

Peer reviewed

HHS Public Access

Author manuscript

J Control Release. Author manuscript; available in PMC 2020 September 10.

Published in final edited form as:

J Control Release. 2019 September 10; 309: 277–288. doi:10.1016/j.jconrel.2019.07.014.

Tumor-specific delivery of gemcitabine with activatable liposomes

Samantha T. Tucci[a,1], **Azadeh Kheirolomoom**[a,b,1], **Elizabeth S. Ingham**[a], **Lisa M. Mahakian**[a], **Sarah M. Tam**[a], **Josquin Foiret**[b], **Neil E. Hubbard**[c], **Alexander D. Borowsky**[c], **Mo Baikoghli**[d], **R. Holland Cheng**[d], **Katherine W. Ferrara**[b,*]

[a]University of California, Davis, Department of Biomedical Engineering, Davis, CA 95616, USA

[b]Stanford University, Department of Radiology, 3165 Porter Drive, Palo Alto, CA 94304, USA

[c]University of California, Davis, Center for Comparative Medicine, Davis, CA 95616, USA

[d]University of California, Davis, Department of Molecular and Cellular Biology, Davis, CA 95616, USA

Abstract

Gemcitabine delivery to pancreatic ductal adenocarcinoma is limited by poor pharmacokinetics, dense fibrosis and hypo-vascularization. Activatable liposomes, with drug release resulting from local heating, enhance serum stability and circulation, and the released drug retains the ability to diffuse within the tumor. A limitation of liposomal gemcitabine has been the low loading efficiency. To address this limitation, we used the superior solubilizing potential of copper(II) gluconate to form a complex with gemcitabine at copper:gemcitabine (1:4). Thermosensitive liposomes composed of DPPC:DSPC:DSPE-PEG2k (80:15:5, mole%) then reached 12 weight % loading, 4-fold greater than previously reported values. Cryo transmission electron microscopy confirmed the presence of a liquid crystalline gemcitabine-copper mixture. The optimized gemcitabine liposomes released 60% and 80% of the gemcitabine within 1 and 5 min, respectively, at 42°C. Liposomal encapsulation resulted in a circulation half-life of ~2 h *in vivo* (compared to reported circulation of 16 min for free gemcitabine in mice), and free drug was not detected within the plasma. The resulting gemcitabine liposomes were efficacious against both murine breast cancer and pancreatic cancer *in vitro.* Three repeated treatments of activatable gemcitabine liposomes plus ultrasound hyperthermia regressed or eliminated tumors in the *neu* deletion model of murine breast cancer with limited toxicity, enhancing survival when compared to treatment with gemcitabine alone. With 5% of the free gemcitabine dose (5 rather than 100 mg/kg), tumor growth was suppressed to the same degree as gemcitabine. Additionally, in a more aggressive tumor

*Corresponding author: Department of Radiology, 3165 Porter Drive, Stanford University, Palo Alto, CA 94304. kwferrar@stanford.edu.

[1]These two authors contributed equally to this work.

Conflict of interest

The authors declare no completing financial of interest.

Supporting Information Available: Additional information for Methods, Supporting information (SI) Table S1 and Figures S1-S6.

model of murine pancreatic cancer, liposomal gemcitabine combined with local hyperthermia induced cell death and regions of apoptosis and necrosis.

Graphical Abstract

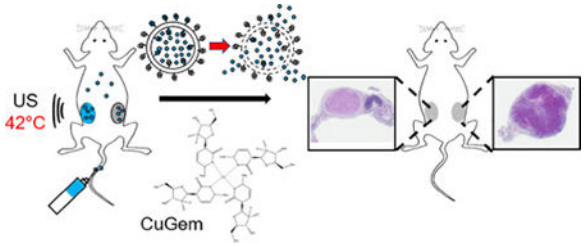

Keywords

Gemcitabine; Temperature-Sensitive Liposome; Ultrasound; Pancreatic Ductal Adenocarcinoma; Breast Cancer

1 Introduction

Pancreatic ductal adenocarcinoma (PDAC) is the most lethal of the major cancers and is projected to remain a leading cause of cancer death from now through 2030 [1–6]. Because approximately 80% of pancreatic cancer patients are not surgical candidates, most patients receive some form of chemotherapy, frequently gemcitabine [7,8] and/or paclitaxel (compounded with albumin to form the nanotherapeutic, Abraxane®), both with limited treatment efficacy [9,10]. Nanotechnological approaches to deliver high doses of chemotherapy to tumors have been successful in both preclinical cancer models and in the clinic [11,12]. Prior to Abraxane's approval for pancreatic cancer in 2013, gemcitabine was the first-line chemotherapeutic, and remains a mainstay of treatment for many patients. Gemcitabine is not currently clinically available in a nanoformulation, although various gemcitabine-containing nanoparticles (NPs) have been evaluated in preclinical studies [11,13–18].

Lipid NPs in general and liposomes in particular are attractive drug delivery platforms due to their biocompatibility and drug encapsulating efficiency. Temperature-sensitive liposomes (TSLs) that can release encapsulated drugs within tumor vasculature in response to hyperthermia can deliver therapeutic doses of free drug to solid tumors [12,19–21]. Importantly, heat-triggered delivery of drug overcomes dependence on passive extravasation of drug-carrying NPs through the enhanced permeation and retention (EPR) effect [22,23]. This method is particularly important for the treatment of pancreatic cancer cells that are surrounded by a dense stroma that prevents drug-carrying NPs from entering the tumor microenvironment. Moreover, the ability to focally target drug release can reduce systemic toxicity.

Gemcitabine is a small water-soluble molecule, as opposed to amphipathic and membrane-permeable anticancer drugs such as doxorubicin (Dox) and irinotecan, and has proven to be difficult to encapsulate in liposomes, with reported concentrations less than 4 weight %

[13,14,17,24,25]. Further, gemcitabine is not a good candidate for remote loading into liposomes using either ammonium sulfate and/or pH gradient or copper gluconate/triethanolamine (Cu/TEOA) gradient methods. Remote loading is a more efficient method compared to passive drug loading, as high intraliposomal concentration of Dox is achieved at drug-to-lipid ratios of 0.05–0.1 and 0.2 (wt/wt) by ammonium sulfate/pH and Cu/TEOA gradient methods, respectively [12,20]. To passively encapsulate gemcitabine in liposomes at such high quantities, both high lipid and drug concentrations are required. Gemcitabine has limited solubility in water or biological buffers such as saline. Both the choice of buffer to maximize gemcitabine solubility and the lipid makeup of the liposome shell can have a significant impact on final drug loading. Further, to stabilize the high payload of drug in liposomes, formation of a drug complex within the core of liposomes can augment loading and reduce drug leakage. We previously reported that formation of a complex between Dox and copper(II) within the core of TSLs stabilizes drug, improves drug pharmacokinetics, and reduces systemic toxicity without affecting drug efficacy [12,26].

Here, we loaded gemcitabine in TSLs (GemTSLs) and incorporated the following strategies to improve the loading and stability of the encapsulated drug: i) we used copper(II) and TEOA to improve gemcitabine solubility and stability when loaded within the core of TSLs and ii) we selected lipid components that permit high gemcitabine loading. The resulting GemTSLs were then characterized with cryo transmission electron microscopy (cryo-EM), and the release kinetics and pharmacokinetics were evaluated. The *in vitro* cytotoxicity of GemTSLs was tested against both murine breast and pancreatic cancer cell types. The anticancer efficacy was studied in the *neu* deletion (NDL) model of murine breast cancer and in murine pancreatic cancer tumor transplants in combination with local hyperthermia. To trigger release of drug in tumors, we employed ultrasound to generate an image-guided and controllable thermal dose [12,19,27,28].

2 Materials and Methods

2.1 Materials

1-Palmitoyl-2-hydroxy-*sn*-glycero-3-phosphocholine (Lyso-PPC), 1-stearoyl-2-hydroxy-*sn*-glycero-3-phosphocholine (Lyso-SPC), 1,2-dipalmitoyl-sn-glycero-3-phosphocholine (DPPC), 1,2-disteraroyl-sn-glycero-3-phosphocholine (DSPC), 1-myristoyl-2-palmitoyl-*sn*-glycero-3-phosphocholine (MPPC), 1-myristoyl-2-stearoyl-*sn*-glycero-3-phosphocholine (MSPC), and 1,2-distearoyl-sn-glycero-3-phosphoethanolamine-N-methoxy polyetheneglycol-2000 (DSPE-PEG2k) were purchased from Avanti Polar Lipids Inc. (Alabaster, AL). Triethanolamine (TEOA) and copper (II) gluconate were purchased from Sigma (St. Louis, MO). Gemcitabine hydrochloride was purchased from LC Laboratories (Woburn, MA).

KPC (mT4) cells were a gift from Dr. David Tuveson (Cold Spring Harbor Laboratory, Cold Spring Harbor, NY). KPC cells were cultured in Dulbecco's Modified Eagle medium (DMEM) containing 4500 mg/L glucose, L-glutamine and sodium pyruvate (# 11995, Invitrogen, San Diego, CA) and supplemented with 10% fetal bovine serum and 1% penicillin–streptomycin. The *neu* deletion (NDL) metastatic mammary carcinoma cell line was a gift from Dr. Alexander Borowsky (University of California- Davis, Davis, CA). NDL

cells were cultured in high-glucose DMEM, supplemented with 10% fetal bovine serum, 1% penicillin-streptomycin, 0.584 g/L L-glutamine and 0.110 g/L sodium pyruvate. All cells were maintained at 37°C in a humidified 5% CO_2 incubator.

2.2 Liposome preparation and drug loading evaluation

Temperature-sensitive liposomes (TSLs) were passively loaded with gemcitabine using lipid film hydration, freeze-thaw, and extruder methods. Lysolipid-containing liposomes were composed of DPPC:Lyso-PPC:DSPE-PEG2k (86:10:4, molar ratio) and DPPC:Lyso-SPC:DSPE-PEG2k (86:10:4). Other liposomes were composed of DPPC:MPPC:DSPE-PEG2k (89:7:4), DPPC:MSPC:DSPE-PEG2k (89:7:4), and DPPC:DSPC:DSPE-PEG2k (80:15:5). Henceforth, with DPPC constituting the core lipid of all liposomal formulation used, each lipid formulation is referred to by its unique lipid component: Lyso-PPC, Lyso-SPC, MPPC, MSPC, and DSPC, respectively, and its gemcitabine content by weight percent.

Briefly, lipids were mixed in chloroform to create a homogenous mixture, and chloroform was slowly evaporated under a stream of nitrogen gas to form a dried lipid film. Residual chloroform was then removed by placing the test tube containing the lipid film in a lyophilizer overnight. Gemcitabine hydrochloride (0, 15, 30, 60, 100, or 150 mg/mL) was mixed in various buffers including saline (pH 5.5), phosphate-buffered saline (PBS, pH 7.4), and Cu(ll) gluconate at 0, 50, 100, and 200 mM Cu plus TEOA at 270 mM at pH 7.4 for at least 5 min at 55°C with vigorous mixing until the solutions were visibly transparent. Dried lipid mixtures were then hydrated with the gemcitabine solutions at 60°C with gentle mixing for 30 min to form gemcitabine liposomes at final lipid concentration of 100 mg/mL. The resulting liposomal gemcitabine solution underwent 4 cycles of freezing in liquid nitrogen (5 min) and thawing at 60°C (7 min) followed by extrusion through a polycarbonate membrane with a 100 nm pore diameter 21 times at 65°C. Liposomes encapsulating gemcitabine were then separated from non-encapsulated gemcitabine and free copper by passing the liposomal solution through a spin column of Sephadex G-75 (5 × 1 cm, GE Healthcare, Biosciences, Piscataway, NJ) equilibrated with saline. Liposome size was then measured using a NICOMP™ 380 ZLS submicron particle analyzer (Particle Sizing System Ince., Santa Barbara, CA). Final lipid concentration was measured using the Phospholipid C assay kit (Wako Chemicals USA, Richmond, VA).

To evaluate gemcitabine loading in liposomes and the efficiency of drug release at 42°C, 35 μL of the purified liposome solution was diluted 4 times in PBS and incubated i) at room temperature (20°C) for 30 min to measure the free gemcitabine (RT), ii) treated with 0.5% Triton™ X-100 (Millipore Sigma, Darmstadt, Germany) at 60°C for 30 min to quantify the total amount of gemcitabine (TX-100), iii) heated to 42°C with gentle mixing for 30 min to assess the release of gemcitabine from liposomes (42°C). The treated solutions were passed through Amicon® Ultra spin filters (30kD MWCO for samples treated Triton X-100 and 100kD MWCO for those incubated samples at RT and 42°C, Millipore Sigma, Darmstadt, Germany) at 2000 × g at 15°C for 30 min to eliminate interference in gemcitabine detection by lipid. The resulting filtrate was measured in triplicate using a NanoDrop ND-1000 Spectrophotometer (Thermo Fisher Scientific, Wilmington, DE) at 271 nm. Gemcitabine

concentration in each liposome formulation was then determined by correlation to standard curves created for gemcitabine in each buffer solution used.

Size and drug leakage from liposomal gemcitabine were monitored for up to one-month upon storage at 4°C post liposome fabrication.

2.3 Copper-gemcitabine complex

Solutions of copper gluconate at 0, 50, 100, and 200 mM copper were made with 270 mM TEOA at pH 7.4 or at 50 mM copper gluconate and absence of TEOA at pH 3.5 or at 50 mM copper gluconate with pH adjusted to 7.4 by NaOH. Each solution was used to dissolve gemcitabine hydrochloride at up to 500 mM at 55°C with vigorous mixing. Each gemcitabine solution was then diluted to 400, 300, 200, 100, and 50 mM gemcitabine with respective buffers. After 12+ h at room temperature or 4°C, each solution was filtered through an A4 filter to remove precipitate and the absorbance of the solution was measured at 271 nm using the NanoDrop ND-1000 Spectrophotometer to assess soluble gemcitabine concentration. Additionally, the absorbance at 650 nm of each solution left at room temperature was measured using a Tecan Infinite® M1000 microplate reader to determine the copper oxidation state.

2.4 Cryo-Electron Microscopy

Cryo-Electron Microscopy Data collection was performed on a JEOL JEM 2100F TEM operating at 200kV. Briefly, a volume of 3 μL solution containing the DSPC-Gem liposomes prepared at initial gemcitabine concentrations of 15, 60, 100, and 150 mg/mL was placed on Quantifoil R2/2 Cu 300 mesh grids. After a 1-minute incubation, 0.5 μm of NP40 detergent was added for 10 seconds. The excess solution was removed and quickly plunged into liquid ethane using FEI Vitrobot Mark III semi-automated cryo-plunger. The liposomes were embedded into a thin layer of vitrified ice and transferred into the EM using a Gatan 626 cryo-transferring system. The grids were examined at 60,000x magnification and images were captured using a D20 detector. The digital images were recorded with a pixel size of 1.4 Å using autofocusing scripts in Serial-EM package, set to defocus level of 0.5–2.5 Å at 60,000x magnification and images were captured using a D20 detector. The digital images with no stigmatism or drift were selected for further analysis and figure preparation.

2.5 Serum stability

A 50% mixture of fetal bovine serum (FBS) in saline was preincubated for 5 min to reach 37°C, 41°C, 42°C, 43°C, or RT. GemTSLs containing copper(II) and gemcitabine were then mixed with the preheated FBS in saline. Samples were taken at 2, 5, 10, and 30 min, cooled on ice, and filtered through Amicon® Ultra spin filters (30kD MWCO) at 2000 × g at 4°C for 30 min. Gemcitabine in the filtrate was measured in triplicate using the NanoDrop ND-1000 Spectrophotometer at 271 nm. Gemcitabine concentration in each liposome formulation was then determined by correlation to standard curves created for gemcitabine in 1:1 FBS:saline.

2.6 Cell viability evaluation

The cytotoxicity of DSPC-based GemTSLs, with and without copper and/or gemcitabine was evaluated *in vitro* in NDL, and KPC (mT4) cell lines for 48h of continuous incubation at various concentrations or after a 20-minute incubation (5 mM) at 37°C or 42°C followed by two rinses and a 48h incubation in media. Following the incubation, MTT (3-(4,5-dimethylthiazol-2-yl)-2,5-diphenyltetrazolium bromide) reagent (Invitrogen Corporation) was added to the medium at 0.5 mg/mL and the cells were incubated for 2 h at 37°C at 5% CO2. Medium was then removed and the formazan crystals were dissolved in 100 μL/well of DMSO (Sigma Aldrich, St. Louis, MO). Absorbance was measured with a Tecan Infinite® M1000 microplate reader.

2.7 Pharmacokinetic analysis

A total of 12 mice (female FVB mice, 8.5 weeks) were studied for pharmacokinetic analysis. DSPC-GemTSLs (loading condition: 100 mg/mL gemcitabine in 100 mM copper(II) plus 270 mM TEOA; 10 wt% gemcitabine) were injected at 20 mg/kg gemcitabine via the tail vein. After 20s, 1h, 2h, and 6h, mice were euthanized via cervical dislocation and blood was harvested (n = 3/timepoint). Collected blood was centrifuged at 1,000 rpm at 4°C for 10 min and plasma was retrieved. Plasma before and after incubation with 0.5% Triton™ X-100 for 30 min at 60°C was passed through Amicon® Ultra spin filters (30kD MWCO) at 2,000 × g at 4°C for 30 min. The resulting filtrate was measured in triplicate using the NanoDrop ND-1000 Spectrophotometer at 271 nm. Free and encapsulated gemcitabine concentrations were determined by correlation to standard curves created for gemcitabine in filtered plasma after spiking gemcitabine at various concentrations into plasma isolated from mouse blood. With this method, we detected gemcitabine in plasma at concentrations as low as 0.025 mg /mL, equivalent to 5% of the initial dose.

2.8 In vivo evaluation

All animal studies were approved by the University of California, Davis Animal Care and Use Committee (IACUC). In efficacy studies, a total of 62 NDL tumor-bearing FVB mice and 27 KPC tumor-bearing C57BL/6 mice were studied. 14 FVB mice were transplanted with unilateral NDL tumors and 48 FVB mice were transplanted with bilateral NDL tumors. C57BL/6 (27) mice were transplanted with unilateral KPC tumors. Once tumor sizes reached ~4 mm, mice were randomized among treatment groups: GemTSLs with ultrasound hyperthermia (GemTSLs+USH), free gemcitabine, saline injection (Saline control).

Briefly, for mice receiving ultrasound hyperthermia, one tumor per animal was insonified for 5 min at 41°C or 42°C (dependent on experimental conditions) prior to the injection of GemTSLs, gemcitabine, or saline via the tail vein. Tumor insonation at 41°C or 42°C continued for an additional 30 min. Treatments occurred 2 times per week for 2–3 treatments and mice were euthanized for histological evaluation 3 days after the last treatment. Treatments occurred 2 times per week for 3 treatments with three to four days interval in survival studies.

The ultrasound system to deliver mild hyperthermia to small murine tumors consisted of a programmable US system combining imaging and therapy (Vantage 256, Verasonics,

Kirkland, WA). A custom 128-element 1.5 MHz therapeutic array was used to heat the tumor [29]. Heating was performed with bursts of 2.5 MPa peak negative pressure, with a pulse repetition frequency of 100 Hz and burst duration ranging from 0 to 8 ms as controlled by a proportional integral derivative (PID) controller (duty cycle ranging from 0 to 0.8) set to maintain the tumor temperature at 42°C. Promptly after necropsy, tumors were fixed in 10% formalin and transferred to 70% ethanol after 24h. Paraffin sections of 4 pm thickness were prepared at the Department of Pathology and Laboratory Medicine, University of California, Davis and stained with Haemotoxylin and Eosin (H&E).

2.9 Statistical analysis

Data points represent the average of multiple measurements (*n* noted in individual figures; n ≥ 3). The error bars represent the standard deviations. One-way ANOVA followed by the Tukey Post Hoc test was used to analyze statistical differences among multiple groups. A p value of less than 0.05 was determined statistically significant.

3 Results

3.1 Initial gemcitabine concentration and liposome shell composition determine loading capacity of gemcitabine liposomes

TSLs were passively loaded with gemcitabine hydrochloride. Multiple components of the gemcitabine-loading conditions were assessed to determine how to maximize the gemcitabine: lipid ratio (wt:wt). In the gemcitabine-containing solution that is added to the dried lipid mixture at elevated temperatures, the concentration of copper(II) gluconate, triethanolamine (TEOA), pH, and gemcitabine chloride concentration were varied. Based on successful active loading of doxorubicin using complexation with copper(II), we hypothesized that copper could positively impact gemcitabine loading. To this end, we used copper(II) gluconate (organic copper salt) and TEOA, a strong base, to form and buffer the copper(II) solution at neutral pH. With 15 mg/mL (50 mM) gemcitabine in the initial loading buffer, the inclusion of copper(II) and/or TEOA resulted in 2–3 weight % loading, and drug loading was negligible for saline or PBS in the absence of copper(II) or TEOA (Figure 1A). The gemcitabine loading in the presence of copper(II) and TEOA was not further enhanced by adjusting copper or TEOA concentrations (SI Figure S1A–B). Additionally, alterations in pH did not impact final gemcitabine content.

When gemcitabine concentration in the loading solution (TEOA 270 mM and copper(II) 100 mM, pH 7.4) was increased to 150 mg/mL, previous loading limits were surpassed, yielding liposomes containing up to 12 weight % (Figure 1B). The gemcitabine loading increased proportionally with the increase in gemcitabine concentration in the loading buffer and the loading efficiency was between 1.5 and 2.5%. The initial solutions were heated to 55°C, allowing gemcitabine to dissolve at higher concentrations than their reported limits (25 mg/mL in water at room temperature per manufacturer's disclosure). Notably, when TEOA and copper(II) were not included, gemcitabine was unable to completely dissolve at elevated temperatures in saline or PBS, suggesting that TEOA and copper interact with gemcitabine to allow for higher drug concentrations to be reached. Using elevated temperature, copper(II)

and TEOA effectively increased gemcitabine solubility, allowing for greater final liposomal gemcitabine content.

Multiple DPPC-based TSL formulations were evaluated, where additional lipids were included at a 7–15% mole ratio with the goal of enhancing the stability or release rate (Table 1). Lipid components studied were either single chain “lyso” lipids (Lyso-PPC or Lyso-SPC) or dual chain lipids (MPPC, MSPC, or DSPC). Loading in lipid formulations containing lyso lipids (typically included to enhance release) was less than ~2 weight %, even at a high initial gemcitabine concentration of 100 mg/mL (SI Figure S1C). In contrast, gemcitabine loading in lipid formulations containing double-chained lipids exceeded 10 weight %.

The resulting GemTSLs have an average diameter of 115 +/− 25 nm and polydispersity index (PDI) of <0.1, which was similar for all formulations tested. Liposomal diameter was monitored for up to one month when stored at 4°C, with no noticeable change in size or PDI. DSPC-GemTSLs containing 10% gemcitabine were stable, with gemcitabine loss into the surrounding buffer less than 3% after 3 weeks at 4°C. Remote gemcitabine loading with varied lipid composition with and without cholesterol using either ammonium sulfate or copper(II) gluconate/TEOA gradient methods was consistently less than that achieved by the passive loading method using copper(II) gluconate/TEOA (SI Figure S1D).

3.2 Copper complexes with gemcitabine, enhancing precipitation

In addition to the increased gemcitabine solubility achieved by copper(II) gluconate, we further explored the interaction between copper and gemcitabine. Solutions of 50 mM copper(II) gluconate and gemcitabine hydrochloride were mixed at varying ratios at 55°C in the presence or absence of 270 mM TEOA at pH 7.4 or 3.5, respectively. After allowing the precipitate to settle at room temperature for 12+ h, the solutions were filtered and the changes in copper absorbance at 650 nm were assessed. At 50 mM copper, pH 7.4 and in the presence of TEOA, the absorbance of copper decreased with increasing gemcitabine (Figure 1C). Once a 4:1 gemcitabine: copper ratio was reached, the absorbance plateaued at 50% maximum absorbance, indicating that up to 4 gemcitabine molecules may interact with a single copper molecule (Figure 1D). The reduction in 650 nm absorbance was not observed in the absence of TEOA at pH 3.5 (SI Figure S2A) or in the presence of TEOA but absence of copper at pH 7.4 (SI Figure S2B). Increasing pH to 7.4 by NaOH in the absence of TEOA partially restored the copper concentration observed at pH 7.4 in the presence of TEOA (SI Figure S2C, Figure 1C). These results suggest that copper complexation with gemcitabine is pH-sensitive, occurs at pH 7.4 and dissociates at pH lower than 7.4 with complete dissociation at pH 3.5. We note that gemcitabine was not soluble at 500 mM in 50 mM copper at pH 3.5 in the absence of TEOA (SI Figure S2A). Although TEOA did not directly interact with gemcitabine, it provided a superior solubilizing effect on gemcitabine and facilitated complex formation between copper and gemcitabine at physiological pH. Drug-copper complexation was not observed during passive loading of gemcitabine at 55–60°C due to the solubilizing effects.

3.3 Cryo transmission electron microscopy of GemTSLs

Cryo transmission electron microscopy (cryo-EM) of DSPC-GemTSLs prepared in the presence of 100 mM copper(II) and 270 mM TEOA at initial gemcitabine concentrations of 15, 60, 100, and 150 mg/mL (corresponding to 2%, 6%, 10%, and 12% drug loading) was obtained (Fig. 2A). Results were compared to DSPC-GemTSLs prepared in the absence of copper and presence of 270 mM TEOA and 100 mg/mL gemcitabine (Fig. 2B). In all gemcitabine concentrations, the majority of liposomes display a single bilayer of 5.5-nm thickness and average size of 100–160 nm (Figure 2C). GemTSLs demonstrated a round morphology at 15 and 60 mg/mL gemcitabine concentration with a trend toward hexagonal morphology at 100 and 150 mg/mL drug concentration. With increasing gemcitabine concentration, the gemcitabine-copper complex was clearly visible in the core of liposomes prepared in the presence of 100 mM copper(II) but not in the core of TSLs prepared in the absence of copper (Figure 2A–B). Viewed by electron microscopy, the image intensity (in arbitrary units) increased from 5.7 in the absence of copper to 15.5 in the presence of 100 mM copper at 100 mg/mL gemcitabine (Figure 2D).

3.4 Serum and plasma stability

DSPC-GemTSLs formed with increasing amounts of gemcitabine (SI Table S1) were incubated in 50% fetal bovine serum at various temperatures. The amount of gemcitabine released from the liposomes was measured over a 30-min time course. DSPC-GemTSLs containing copper and 2% to 10% gemcitabine were largely stable in serum at 37 °C, releasing <25% of the drug within 5 min and 40% and 30% within 30 min at 2% and 6–10% gemcitabine, respectively (Fig. 3A–B, SI Fig. S3A–B; blue lines). DSPC-GemTSLs with 12% gemcitabine (DSPC-GemTSLs-12%) released ~50% of encapsulated drug within 5 min of serum incubation at 37 °C (Fig. 3C, blue line). At 42 °C (the phase transition temperature of the core lipid DPPC) all formulations released 80–100% of their encapsulated drug after 30 min. Increasing the loaded mass of gemcitabine led to more rapid release, likely because of higher internal osmotic pressure. After 5 min at 42 °C, DSPC-GemTSLs-2% released ~60% drug content, DSPC-GemTSLs-6% released ~90% drug content, DSPC-GemTSLs-10% released ~80% drug content, and DSPC-GemTSLs-12% released 100% of the drug content. The lower drug release rate observed for DSPC-GemTSLs-10% at 37 °C and 42 °C is likely due to the reduced internal osmotic pressure induced by formation of the copper-drug complex at 1:4 mol ratio. In the absence of copper and presence of 270 mM TEOA, the maximum loading was 8% for 100 mg/mL gemcitabine (DSPC-GemTSLs-8%) compared to 10% achieved in the presence of 100 mM copper and 270 mM TEOA. Despite the lower drug loading, the copper-free formulation at 37 °C released ~40% gemcitabine within 5 min and ~80% gemcitabine after 30 min, suggesting copper plays a stabilizing role (Fig. 3D). Compared to DSPC-GemTSLs displaying robust serum stability with 2–10% gemcitabine release at 37 °C, the alternative TSL formulation, MPPC-GemTSLs, showing >70% drug release at 42 °C within 5 min, was stable only at 2% gemcitabine at 37 °C (SI Fig. S3C).

The release profiles of the liposomes were evaluated at 41 °C and 43°C to determine the *in vivo* heating conditions most likely to release the highest dose of gemcitabine in a locally-heated tumor. DSPC-GemTSLs-10% showed ~ 2-fold higher release of drug within 5 min at

42°C compared to 41 °C (Figure 3A). Most importantly, ~60 and 70% of the drug was released within 1 minute at 42 and 43°C, respectively (Figure 3B). For tumors with a diameter of 1 cm or greater, this 1-minute release will be important to increase deposition within the tumor. Within a 30-sec incubation at 43°C, drug release increased 3-fold and 2-fold after 10 and 20–30 sec, respectively, compared to the release at 42°C (Figure 3B). However, for safety concerns in small animal models, we employed ultrasound-hyperthermia at 42°C for local release of gemcitabine from DSPC-GemTSLs-10%.

The pharmacokinetics of DSPC-GemTSLs-10% were assessed in healthy FVB mice by measuring the plasma concentration of liposomal and unencapsulated gemcitabine over a 6h time course (Figure 3E) using a gemcitabine standard curve generated from spiking varying amounts of gemcitabine in plasma isolated from mouse blood (SI Figure S3D). The half-life of liposomal gemcitabine was 2.01 h and the level of unencapsulated gemcitabine remained low over 6 h of circulation, indicating that DSPC-GemTSLs-10% were stable. Therefore, based on the favorable stability and release profiles of the DSPC-GemTSLs-10%, in all following studies, these TSLs were used and further abbreviated to GemTSLs unless otherwise stated.

3.5 Copper-gemcitabine liposomes show in vitro efficacy against breast cancer and pancreatic cancer cell lines

The mT4 cell line, derived from the genetically-engineered KPC ($Kras^{LSL\text{-}G12D/+}$; $Trp53^{LSL\text{-}R172H/+}$; Pdx-Cre) mouse model of pancreatic cancer, was found to display strong sensitivity to gemcitabine with a half-maximal inhibitory concentration (IC50) of 9.4 ± 0.4 nM. Gemcitabine cytotoxicity was also evaluated in a syngeneic, orthotopic murine model of epithelial mammary adenocarcinoma, the *neu* exon deletion (NDL) cell line [30,31], which had an IC50 value of 20 ± 1 nM.

Both KPC and NDL cells showed a near identical dose response to GemTSLs and free gemcitabine, with no cytotoxicity from an equimolar lipid dosing of empty DSPC-TSLs-0% (Figure 4A–B). Heating to 42°C for 20 min to mimic the *in vivo* conditions of ultrasound hyperthermia (USH) followed by a continuous 48 h incubation with gemcitabine or GemTSLs did not confer additional cytotoxicity (Figure 4A–B).

When KPC and NDL cells were exposed to GemTSLs at a high dose (5 mM) for 20 min at 42°C and subsequently washed, there was a significant decrease in cell viability compared to those cells incubated at 37°C (60% vs 45% for KPC and 68% vs 60% for NDL) (Figure 4C–D). No temperature effect was detected with free gemcitabine, empty DSPC-TSLs-0%, or no treatment controls. We anticipated that a significant toxicity would be observed if liposomes were present on tumor cells at the same concentration as the free drug (with or without a temperature increase). This was the result for the studies reported here. However, in pancreatic cancer, the liposomes are unlikely to contact tumor cells *in vivo* at the same concentration as free drug as the EPR effect is weak.

3.6 Copper-gemcitabine liposomes plus ultrasound hyperthermia suppressed tumor growth in syngeneic murine models of pancreatic and breast cancer

In mice bearing either unilateral or bilateral NDL tumors, GemTSLs were evaluated at 10 mg/kg gemcitabine plus USH with a peak temperature of 42°C. A 2D phased array transducer was programmed to distribute energy with a −3 dB and −6 dB intensity of ~2.5 mm and 5 mm in diameter, respectively (SI Figure S4A–B). In unilateral NDL-bearing mice, the growth of directly-heated tumors treated with GemTSLs was suppressed compared to both gemcitabine (10 mg/kg) and saline-treated tumors (Figure 5A). Similar results were found in the bilateral NDL-tumor model (Figure 5B). In bilateral NDL-bearing mice, the histology of tumors directly heated and treated with GemTSLs after three treatments on day 36 showed the potential to eliminate all viable tumor (Figure 5C). The tumors contralateral to the directly-heated tumors showed large areas of non-adherent and apoptotic tumor cells, though most of the tumor cells remained viable (Figure 5D). Gemcitabine-treated tumors were mostly viable but contained some necrotic areas (Figure 5E) while saline-injected control tumors remained highly-viable (Figure 5F).

Over the course of the treatment, DSPC-GemTSLs-10% treated mice lost weight following each USH session but recovered after a few days (SI Figure S5A). Final organ weights of DSPC-GemTSLs-10% treated animals were not significantly different than gemcitabine or saline control treated animals (SI Figure S5B).

MPPC-GemTSLs-2% at 5 mg/kg gemcitabine were also evaluated, but due to lower drug loading efficiency, the gemcitabine dose was limited to prevent confounding toxicity from the high lipid content. When combined with USH at 41°C, MPPC-GemTSLs-2% at 5 mg/kg gemcitabine reduced tumor growth to a level equivalent to 20x the dose of free gemcitabine (100 mg/kg; Figure 5G). Tumor growth suppression was less than that achieved with the DSPC-GemTSLs-10% formulation. Both groups of mice receiving gemcitabine-containing treatments lost an average of 10% body weight over the course of treatment and experienced splenomegaly (SI Figure S5C–D). Throughout the treatment course, mice receiving gemcitabine at 100 mg/kg experienced diarrhea. Despite limited efficacy against tumor growth and the above-observed toxicities, both the directly-heated tumor (Figure 5H) and contralateral tumor (Figure 5I) receiving MPPC-GemTSLs-2% had clear areas of nonviable tumor cells, while the free-gemcitabine treated (Figure 5J) and saline control tumors (Figure 5K) remained largely viable.

GemTSLs were also evaluated at 10 mg/kg gemcitabine plus USH in mice with KPC pancreatic tumors transplanted into the mammary fat pad. Tumor viability was reduced in directly-heated tumors as compared with control tumors. An antivascular effect (as previously reported for doxorubicin [12]) was evident, with hemorrhage observed in the treated volume (Figure 6A–C).

In this model, tumor growth of the directly-heated tumors treated with GemTSLs was not significantly suppressed compared to either gemcitabine or saline (SI Figure S6A). Over the course of the treatment, GemTSL-treated mice lost weight, although final organ weights of GemTSL-treated animals were not significantly different than free gemcitabine or saline-control treated animals (SI Figure S6B–C). In addition, KPC tumors invade the abdomen,

rapidly growing through the abdominal wall (SI Figure S6D). Treatment of this area resulted in a high concentration of gemcitabine in the intestinal tract and significant toxicity, and therefore was discontinued. In studies of larger animals or human treatment, the relatively lower tumor growth rate and safer spatial distance between organs would allow for a longer treatment course.

4 Discussion

Here, we present thermally-activatable liposomes containing gemcitabine and demonstrate their efficacy. With a 12% (wt/wt) formulation, the loading exceeded that previously reported (~2–4% wt/wt) [11,17,32]. Three treatments involving release of drug from these particles was sufficient to eliminate or greatly reduce viable tumor in gemcitabine-sensitive breast tumors in mice. Growth of the distant tumors was also suppressed, likely as a result of the drug accumulation. MPPC-based liposomes were stably loaded with 2% (wt/wt) gemcitabine. With 5% of the free gemcitabine dose (5 rather than 100 mg/kg), tumor growth was suppressed to the same degree as gemcitabine. Thus, we found that with the TSLs, the systemic gemcitabine dose could be reduced 20-fold or more with a similar or improved efficacy. This likely results both from greater concentration and the ability of the lipid shell to shield gemcitabine from rapid deactivation in the blood and deliver still-potent gemcitabine. Dosed at 20 mg/kg in healthy mice in the absence of USH, DSPC-GemTSLs-10% circulated with a half-life of 2.01h compared to free gemcitabine with a short plasma half-life of 8–17 min in mice [33]. Free gemcitabine was undetectable in plasma throughout the time course, suggesting minimal un-triggered release of gemcitabine from the liposomes while in circulation.

To evaluate *in vivo* efficacy in a pancreatic cancer model, we created a superficial pancreatic tumor model through implantation of KPC cells into the mammary fat pads of C57BL/6 mice. The resulting tumors retained the ductal, dense stromal and highly-invasive characteristics of pancreatic cancer, and allowed for US treatment to increase temperature while minimizing skin damage. Here again, USH-triggered release of gemcitabine led to decreased cell viability within the treated tumors and, in some, areas of dysfunctional endothelium resulting in local hemorrhage. Upon histopathology, we found that large regions of the treated tumors were no longer viable. The highly-invasive KPC tumors limited our treatment window to 2 treatments due to tumor invasion of the abdomen. Due to the invasion, image-guided treatment of the tumors then resulted in intestinal toxicity due to the close proximity of the tumor and intestine. Particularly in small rodents, a significant fraction of the intestine is within a few millimeters of the tumor and limits continued treatment. When combined with USH to trigger drug release in tumor vasculature, the activatable liposomes deposited free drug; however, we were not able to quantify the drug concentration within the tumor after treatment due to rapid drug degradation, although we continue to seek a quantitative methodology in our ongoing work.

Gemcitabine-loaded temperature-sensitive liposomes could enhance current therapy options, offering a strategy to target drug delivery and limit systemic toxicity. As shown here, the KPC cell line is highly responsive to gemcitabine *in vitro,* but the fast-growing *in vivo* models prove much more challenging to treat. Improving efficacy may require more

aggressive dosing or combinations of chemotherapeutics to out-pace tumor growth. Based on the relative success of the MPACT trial, combinations of gemcitabine liposomes with Abraxane could lead to more meaningful responses and the lower toxicity profiles may expand the number of patients who could tolerate such an aggressive regimen. Preclinically, gemcitabine liposomes combined with nanoformulations of paclitaxel have been successful in *in vivo* cancer models. The loading methodology reported here provides opportunity to co-deliver other anticancer agents passively or remotely loaded to the same liposomes.

The drug loading methodology reported here augments drug solubility with a copper-containing buffer which further results in a copper-drug complex within the liposomes. Additionally, the lipid formulation is adapted to minimize interaction with gemcitabine. Together, these techniques enable the fabrication of stable, high-content GemTSLs. Creating gemcitabine liposomes with a high mass loading has been challenging, as conventional methods of loading drugs into liposomes have yielded low drug loading by weight. To passively load gemcitabine into liposomes in significant quantities, a high concentration of gemcitabine must be achieved in the initial loading buffer, as the inner liposome solution will be roughly equivalent to the initial loading buffer. Using a combination of copper(II) gluconate, TEOA, and heat, gemcitabine became soluble up to 150 mg/mL. We previously demonstrated that forming a complex between copper(II) and Dox reduced drug leakage in plasma, improved drug pharmacokinetics and enabled chemotherapeutic efficacy with minimal toxicity [12,26,34]. To this end, we explored the possibility of interaction between copper and gemcitabine and found that a combination of copper(II) gluconate with TEOA buffer has a superior potential in solubilizing gemcitabine, which otherwise could not be obtained by saline or PBS buffer.

The liposome shell components are also important factors in gemcitabine loading. Although lyso lipids are attractive for use in TSLs due to their ability to rapidly release drug cargo, gemcitabine loading was less than 2%. Previous reports indicate that lipid composition affects the physical-chemical properties and biological activity of gemcitabine liposomes [35] and that gemcitabine interacts with certain phospholipids [36]. We found that liposome shells comprised entirely of dual-chained lipids enhanced gemcitabine loading. To this end, liposomes composed primarily of DPPC (phase transition of 42°C) DSPC, and DSPE-PEG2k were used.

Formation of a complex between copper and gemcitabine within the core of liposomes stabilized gemcitabine. Copper-drug complexes can alter both physiochemical properties of liposomes [12,26] and biological drug interactions [26,34,37,38]. Thus, we probed copper's interaction with gemcitabine—a cytidine analogue—to find that it complexes in a 1:4 ratio. Copper has been reported to interact with N(3) of cytidine in a 1:4 complex, suggesting that copper may interact with gemcitabine in a similar conformation [39,40]. Moreover, we observed the unique copper-gemcitabine complex within TSLs using cryo-EM. Increasing the amount of internal gemcitabine led to increased signal intensity within the core of liposomes containing copper and caused morphology to shift from spherical to a hexagonal liposome structure. While the payload EM intensity was quantified as 5.7 (arbitrary units) within TSLs prepared in the absence of copper, the value increased to 15.5 in the presence of

copper at 100 mg/mL gemcitabine and a gemcitabine-copper complex was visible within the core of TSLs.

Although TSLs could be formulated at up to 12% gemcitabine, serum stability decreased with increasing gemcitabine loading. Loading of 10% gemcitabine resulted in ~30% of gemcitabine leakage after 30 min at 37°C. For reference, approximately 50% of doxorubicin is released from temperature sensitive liposomes after 1 h of circulation *in vivo* [41,42]. In serum, the rate of drug release increased with increasing temperature, and 42°C was chosen as the release temperature for *in vivo* studies to balance rapid drug release with limited thermal dose. Locally-activatable gemcitabine-filled nanoparticles allow higher doses of drug to be released in the tumor, limiting off-target effects and increasing antitumor efficacy. DSPC-GemTSLs-10% combined with USH suppressed tumor growth and led to significant tumor cell death in the focally-heated region.

5 Conclusions

We developed a novel method for local delivery of high gemcitabine content liposomes stabilized with copper and activatable with ultrasound hyperthermia. The interaction of copper with gemcitabine is critical for obtaining the high concentration of gemcitabine in the loading buffers which led to passive loading of gemcitabine at concentrations 4x what has been previously reported. Our high-capacity temperature sensitive liposomes suppressed tumor growth in murine models of breast cancer and reduced pancreatic tumor cell viability with minimal systemic toxicity.

Supplementary Material

Refer to Web version on PubMed Central for supplementary material.

Acknowledgements

This work was supported by funding from National Institute of Health grants NIHR01CA112356, NIHR01CA134659, NIHR01CA199658, NIHR01CA210553 and NIHR01CA211602.

References

[1]. Rahib L, Smith BD, Aizenberg R, Rosenzweig AB, Fleshman JM, Matrisian LM, Projecting Cancer Incidence and Deaths to 2030: The Unexpected Burden of Thyroid, Liver, and Pancreas Cancers in the United States, Cancer Res. 74 (2014) 4006. doi: 10.1158/0008-5472.Can-14-1642.

[2]. Adamska A, Domenichini A, Falasca M, Pancreatic ductal adenocarcinoma: Current and evolving therapies, Int. J. Mol. Sci 18 (2017). doi:10.3390/ijms18071338.

[3]. Becker AE, Hernandez YG, Frucht H, Lucas AL, Pancreatic ductal adenocarcinoma: Risk factors, screening, and early detection, World J. Gastroenterol 20 (2014) 11182–11198. doi:10.3748/wjg.v20.i32.11182. [PubMed: 25170203]

[4]. Foucher ED, Ghigo C, Chouaib S, Galon J, lovanna J, Olive D, Pancreatic ductal adenocarcinoma: A strong imbalance of good and bad immunological cops in the tumor microenvironment, Front. Immunol 9 (2018) 1–8. doi:10.3389/fimmu.2018.01044. [PubMed: 29403488]

[5]. Hezel AF, Kimmelman AC, Stanger BZ, Bardeesy N, Depinho R. a, Genetics and biology of pancreatic ductal adenocarcinoma Genetics and biology of pancreatic ductal adenocarcinoma, Cold Spring Harb. Lab. Press 1 (2006) 1218–1249. doi:10.1101/gad.1415606.

[6]. Cid-Arregui A, Juarez V, Perspectives in the treatment of pancreatic adenocarcinoma, World J. Gastroenterol 21 (2015) 9297–9316. doi:10.3748/wjg.v21.i31.9297. [PubMed: 26309356]

[7]. Iosune PM, Jaime B, Aramend JM, Fern OA, Santisteban M, Combination of pegylated liposomal doxorubicin plus gemcitabine in heavily pretreated metastatic breast cancer patients: Long-term results from a single institution experience, Breast J (2017) 473–479. doi:10.1111/tbj.12975. [PubMed: 29286192]

[8]. Fleeman N, Abdulla A, Bagust A, Beale S, Richardson M, Stainthorpe A, Boland A, Kotas E, Mcentee J, Palmer D, Pegylated liposomal irinotecan hydrochloride trihydrate for treating pancreatic cancer after gemcitabine: An evidence review group perspective of a NICE Single Technology Appraisal, Pharmacoeconomics 36 (2018) 289–299. doi:10.1007/s40273-017-0592-3. [PubMed: 29178025]

[9]. Tahara J, Shimizu K, Otsuka N, Akao J, Takayama Y, Tokushige K, Gemcitabine plus nab-paclitaxel vs. FOLFIRINOX for patients with advanced pancreatic cancer, Cancer Chemother. Pharmacol 82 (2018) 245–250. doi:10.1007/s00280-018-3611-y. [PubMed: 29846765]

[10]. Von Hoff DD, Ervin T, Arena FP, Chiorean EG, Infante J, Moore M, Seay T, Tjulandin SA, Ma WW, Saleh MN, Harris M, Reni M, Dowden S, Laheru D, Bahary N, Ramanathan RK, Tabernero J, Hidalgo M, Goldstein D, Van Cutsem E, Wei X, Iglesias J, Renschler MF, Increased Survival in Pancreatic Cancer with nab-Paclitaxel plus Gemcitabine, N. Engl. J. Med 369 (2013) 1691–1703. doi:10.1056/NEJMoa1304369. [PubMed: 24131140]

[11]. May JP, Ernsting MJ, Undzys E, Li SD, Thermosensitive Liposomes for the Delivery of Gemcitabine and Oxaliplatin to Tumors, Mol. Pharm 10 (2013) 4499–4508. doi:10.1021/mp400321e. [PubMed: 24152292]

[12]. Kheirolomoom A, Lai CY, Tam SM, Mahakian LM, Ingham ES, Watson KD, Ferrara KW, Complete regression of local cancer using temperature-sensitive liposomes combined with ultrasound-mediated hyperthermia, J. Control. Release 172 (2013) 266–273. doi:10.1016/j.jconrel.2013.08.019. [PubMed: 23994755]

[13]. Papa AL, Basu S, Sengupta P, Banerjee D, Sengupta S, Harfouche R, Mechanistic studies of Gemcitabine-loaded nanoplatforms in resistant pancreatic cancer cells, BMC Cancer. 12 (2012) 419. doi:10.1186/1471-2407-12-419. [PubMed: 22998550]

[14]. Papa AL, Sidiqui A, Balasubramanian SUA, Sarangi S, Luchette M, Sengupta S, Harfouche R, PEGylated liposomal Gemcitabine: insights into a potential breast cancer therapeutic, Cell. Oncol 36 (2013) 449–457. doi:10.1007/s13402-013-0146-4.

[15]. Fuse T, Tagami T, Tane M, Ozeki T, Effective light-triggered contents release from helper lipid-incorporated liposomes co-encapsulating gemcitabine and a water-soluble photosensitizer, Int. J. Pharm 540 (2018) 50–56. doi:10.1016/j.ijpharm.2018.01.040. [PubMed: 29410222]

[16]. Cosco D, Bulotta A, Ventura M, Celia C, Calimeri T, Perri G, Paolino D, Costa N, Neri P, Tagliaferri P, Tassone P, Fresta M, In vivo activity of gemcitabine-loaded PEGylated small unilamellar liposomes against pancreatic cancer, Cancer Chemother. Pharmacol 64 (2009) 1009–1020. doi:10.1007/s00280-009-0957-1. [PubMed: 19263052]

[17]. Xu HT, Paxton J, Lim J, Li Y, Zhang WL, Duxfield L, Wu ZM, Development of High-Content Gemcitabine PEGylated Liposomes and Their Cytotoxicity on Drug-Resistant Pancreatic Tumour Cells, Pharm. Res 31 (2014) 2583–2592. doi:10.1007/s11095-014-1353-z. [PubMed: 24639234]

[18]. Calvagno M. Grazia, Celia C, Paolino D, Cosco D, Iannone M, Castelli F, Doldo P, Fresta M, Effects of Lipid Composition and Preparation Conditions on Physical-Chemical Properties, Technological Parameters and In Vitro Biological Activity of Gemcitabine-Loaded Liposomes, Curr. Drug Deliv 4 (2006) 89–101. doi:10.2174/156720107779314749.

[19]. Li L, ten Hagen TLM, Hossann M, Suss R, van Rhoon GC, Eggermont AMM, Haemmerich D, Koning GA, Mild hyperthermia triggered doxorubicin release from optimized stealth thermosensitive liposomes improves intratumoral drug delivery and efficacy, J. Control. Release 168 (2013) 142–150. doi:10.1016/j.jconrel.2013.03.011. [PubMed: 23524188]

[20]. de Smet M, Langereis S, van den Bosch S, Grull H, Temperature-sensitive liposomes for doxorubicin delivery under MRI guidance, J Control Release. 143 (2010) 120–127. doi:10.1016/j.jconrel.2009.12.002. [PubMed: 19969035]

[21]. Chiu GNC, Abraham SA, Ickenstein LM, Ng R, Karlsson G, Edwards K, Wasan EK, Bally MB, Encapsulation of doxorubicin into thermosensitive liposomes via complexation with the

transition metal manganese, J. Control. Release 104 (2005) 271–288. doi:10.1016/j.cornel.2005.02.009. [PubMed: 15907579]

[22]. Maeda H, The enhanced permeability and retention (EPR) effect in tumor vasculature: The key role of tumor-selective macromolecular drug targeting, in: Weber G (Ed.), Adv. Enzym. Regul Vol 41, Pergamon-Elsevier Science Ltd, Oxford, 2001: pp. 189–207.

[23]. Kobayashi H, Watanabe R, Choyke PL, Dahlin A, Improving conventional enhanced permeability and retention (EPR) effects; What is the appropriate target?, Publications.Uu.Se 4 (2005) 2–25. doi:10.7150/thno.7193.

[24]. Bersani S, Vila-caballer M, Brazzale C, Barattin M, Salmaso S, European Journal of Pharmaceutics and Biopharmaceutics decorated liposomes for the delivery of gemcitabine to cancer cells, Eur. J. Pharm. Biopharm 88 (2014) 670–682. doi:10.1016/j.ejpb.2014.08.005. [PubMed: 25157908]

[25]. Liu Y, Tamam H, Yeo Y, P. AAPS PharmSciTech (2018) 19: 693–699. doi:10.1208/s12249-017-0877-z.

[26]. Kheirolomoom A, Mahakian LM, Lai CY, Lindfors HA, Seo JW, Paoli EE, Watson KD, Haynam EM, Ingham ES, Xing L, Cheng RH, Borowsky AD, Cardiff RD, Ferrara KW, Copper-Doxorubicin as a Nanoparticle Cargo Retains Efficacy with Minimal Toxicity, Mol. Pharm 7 (2010) 1948–1958. doi:10.1021/mp100245u. [PubMed: 20925429]

[27]. Wong AW, Fite BZ, Liu Y, Kheirolomoom A, Seo JW, Watson KD, Mahakian LM, Tam SM, Zhang H, Foiret J, Borowsky AD, Ferrara KW, Ultrasound ablation enhances drug accumulation and survival in mammary carcinoma models, J. Clin. Invest 126 (2016) 99–111. doi:10.1172/jci83312. [PubMed: 26595815]

[28]. Gasselhuber A, Dreher MR, Partanen A, Yarmolenko PS, Woods D, Wood BJ, Haemmerich D, Targeted drug delivery by high intensity focused ultrasound mediated hyperthermia combined with temperature-sensitive liposomes: Computational modelling and preliminary in vivovalidation, Int. J. Hyperth 28 (2012) 337–348. doi: 10.3109/02656736.2012.677930.

[29]. Liu JF, Foiret J, Stephens DN, Le Baron O, Ferrara KW, Development of a spherically focused phased array transducer for ultrasonic image-guided hyperthermia, Phys. Med. Biol 61 (2016) 5275–5296. doi:10.1088/0031-9155/61/14/5275. [PubMed: 27353347]

[30]. Borowsky AD, Namba R, Young LJT, Hunter KW, Hodgson JG, Tepper CG, McGoldrick ET, Muller WJ, Cardiff R, Gregg JP, Syngeneic mouse mammary carcinoma cell lines: Two closely related cell lines with divergent metastatic behavior, Clin. Exp. Metastasis 22 (2005) 47–58. doi: 10.1007/s10585-005-2908-5. [PubMed: 16132578]

[31]. Cardiff RD, Hubbard NE, Engelberg JA, Munn RJ, Miller CH, Walls JE, Chen JQ, Velasquez-Garcia HA, Galvez JJ, Bell KJ, Beckett LA, Li YJ, Borowsky AD, Quantitation of fixative-induced morphologic and antigenic variation in mouse and human breast cancers, Lab. Investig 93 (2013) 480–497. doi:10.1038/labinvest.2013.10. [PubMed: 23399853]

[32]. Zhang Y, Bush X, Yan B, Chen JA, Gemcitabine nanoparticles promote antitumor immunity against melanoma, Biomaterials. 189 (2019) 48–59. doi:10.1016/j.biomaterials.2018.10.022. [PubMed: 30388589]

[33]. Brusa P, Immordino ML, Rocco F, Cattel L, Antitumor activity and pharmacokinetics of liposomes containing lipophilic gemcitabine prodrugs, Anticancer Res. 27 (2007) 195–200. [PubMed: 17352232]

[34]. Kheirolomoom A, Ingham ES, Commisso J, Abushaban N, Ferrara KW, Intracellular trafficking of a pH-responsive drug metal complex, J. Control. Release 243 (2016) 232–242. doi:10.1016/j.jconrel.2016.10.012. [PubMed: 27746275]

[35]. Calvagno MG, Celia C, Paolino D, Cosco D, Iannone M, Castelli F, Doldo P, Frest M, Effects of lipid composition and preparation conditions on physical-chemical properties, technological parameters and in vitro biological activity of gemcitabine-loaded liposomes, Curr Drug Deliv. 4 (2007) 89–101. [PubMed: 17269921]

[36]. Castelli F, Raudino A, Fresta M, A mechanistic study of the permeation kinetics through biomembrane models: gemcitabine-phospholipid bilayer interaction, J Colloid Interface Sci. 285 (2005) 110–117. doi:10.1016/j.jcis.2004.11.039. [PubMed: 15797403]

[37]. Iakovidis I, Delimaris I, Piperakis SM, Copper and its complexes in medicine: a biochemical approach, Mol Biol Int. 2011 (2011) 594529. doi:10.4061/2011/594529. [PubMed: 22091409]

[38]. Greenaway FT, Dabrowiak JC, The Binding of Copper Ions to Daunomycin and Adriamycin, J. Inorg. Biochem 16 (1982) 91–107.

[39]. Kinjo Y, Ji LN, Corfu NA, Sigel H, Ambivalent Metal-Ion Binding-Properties of Cytidine in Aqueous-Solution, Inorg. Chem. 31 (1992) 5588–5596. doi:DOI 10.1021/ic00052a039.

[40]. Palaniandavar M, Somasundaram I, Lakshminarayanan M, Manohar H, Stabilisation of unusual simultaneous binding of four cytosine nucleobases to copper(II) by a novel network of bifurcated hydrogen bonding, J. Chem. Soc. Trans (1996) 1333–1340. doi:DOI 10.1039/dt9960001333.

[41]. Tagami T, May JP, Ernsting MJ, Li S, A thermosensitive liposome prepared with a Cu 2 + gradient demonstrates improved pharmacokinetics, drug delivery and antitumor ef fi cacy, J. Control. Release 161 (2012) 142–149. doi:10.1016/j.jconrel.2012.03.023. [PubMed: 22504351]

[42]. Dicheva BM, Seynhaeve ALB, Soulie T, Eggermont AMM, Ten Hagen TLM, Koning GA, Pharmacokinetics, Tissue Distribution and Therapeutic Effect of Cationic Thermosensitive Liposomal Doxorubicin Upon Mild Hyperthermia, Pharm. Res 33 (2016) 627–638. doi:10.1007/s11095-015-1815-y. [PubMed: 26518763]

Highlights

- Gemcitabine was solubilized up to 150 mg/mL in the presence of copper and TEOA
- Gemcitabine was stably loaded into thermally-activatable liposomes at 12 wt/wt%
- 60–70% of drug was released from activatable liposomes within 1 min at 42–43°C
- Liposomal gemcitabine had equivalent toxicity to free drug in pancreatic cancer cells
- Liposomal gemcitabine activated with ultrasound reduced tumor viability

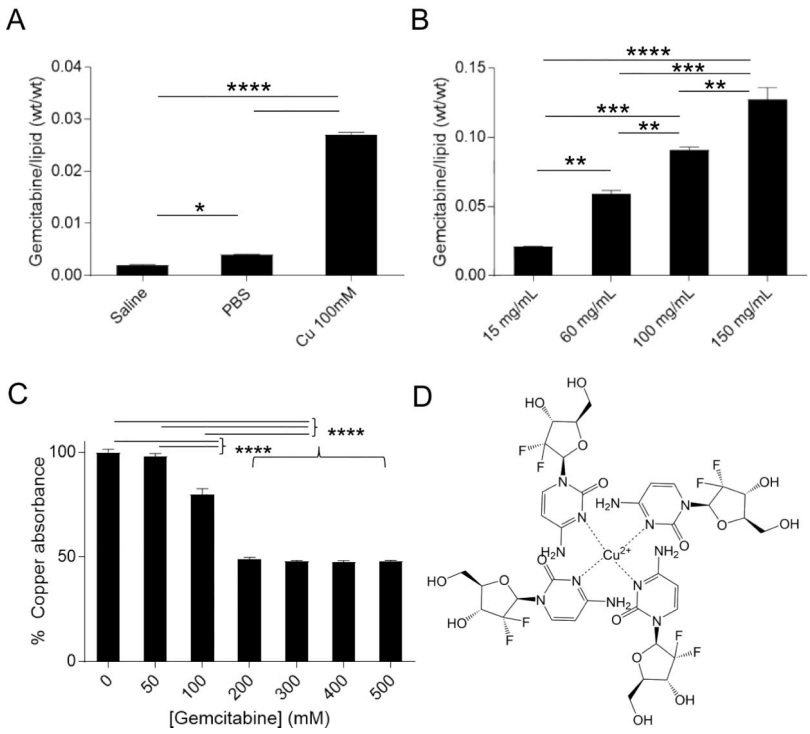

Figure 1. Optimization of gemcitabine loading with copper-containing buffer.

(A) Gemcitabine loading (measured as gemcitabine/lipid (wt/wt) as a function of loading buffers with and without copper(II) (Cu) gluconate and (B) initial gemcitabine hydrochloride concentration in the loading buffer. (C) The 650 nm absorbance of copper at 50 mM (with TEOA 270 mM, pH 7.4) was measured in the presence of increasing amounts of gemcitabine. (D) Structure of copper(II) complexed with four gemcitabine molecules. All lipid shells were comprised of DPPC:DSPC:DSPE-PEG2k (80:15:5, molar ratio). Statistical analyses consisted of a 1-way ANOVA followed by the Tukey Post Hoc test. * $p < 0.05$; ** $p < 0.01$; *** $p < 0.001$; **** $p < 0.0001$.

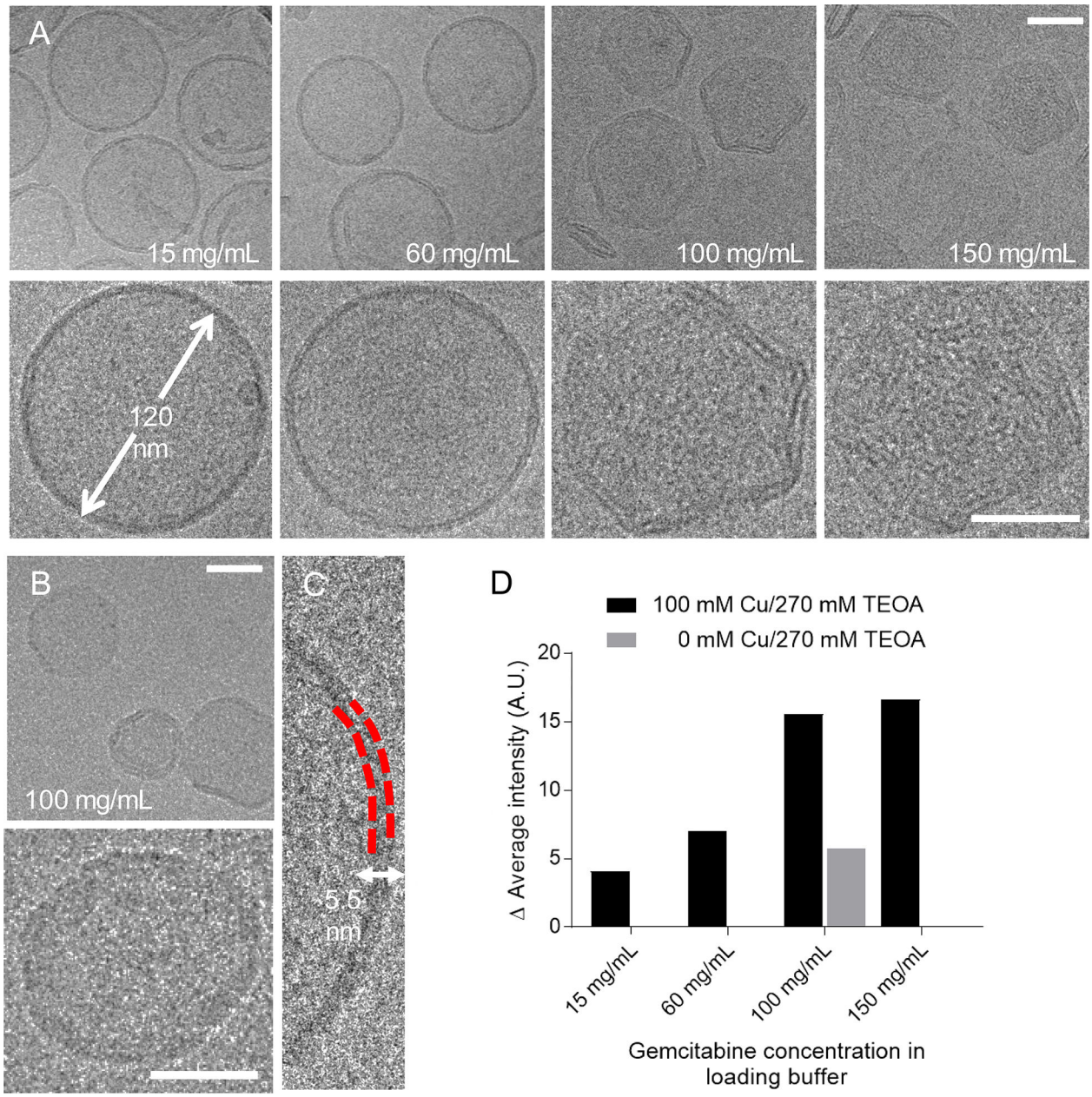

Figure 2. Cryo-electron microscopy of gemcitabine-loaded liposomes.

(A) Field view (top) and individual particles (bottom) of gemcitabine-loaded TSLs prepared with gemcitabine at 15, 60, 100, and 150 mg/mL in 100 mM copper(II) gluconate and 270 mM TEOA in the loading buffer, from left to right and (B) when prepared in the absence of copper(II) and 270 mM TEOA at gemcitabine concentration of 100 mg/mL. Average diameter of the TSLs was measured at 120 ± 30.75 nm. (C) Magnified view of liposomal bilayer measured to be 5.5 nm in thickness. (D) Quantitative average intensity analysis to measure payload with respect to increasing gemcitabine concentrations in the presence or absence of 100 mM copper(II) (Cu) gluconate in the loading buffer containing 270 mM TEOA. The intensity measurements in (D) represent the difference between the intensity

inside and outside each particle averaged over at least 5 particles with each gemcitabine concentration. Due to the near-zero values of the standard deviation, error bars are not visible in (D). Scale bars in A and B represent 100 and 50 nm for the top and bottom EM images, respectively. A.U. arbitrary units. All lipid shells were comprised of DPPC:DSPC:DSPE-PEG2k (80:15:5, molar ratio).

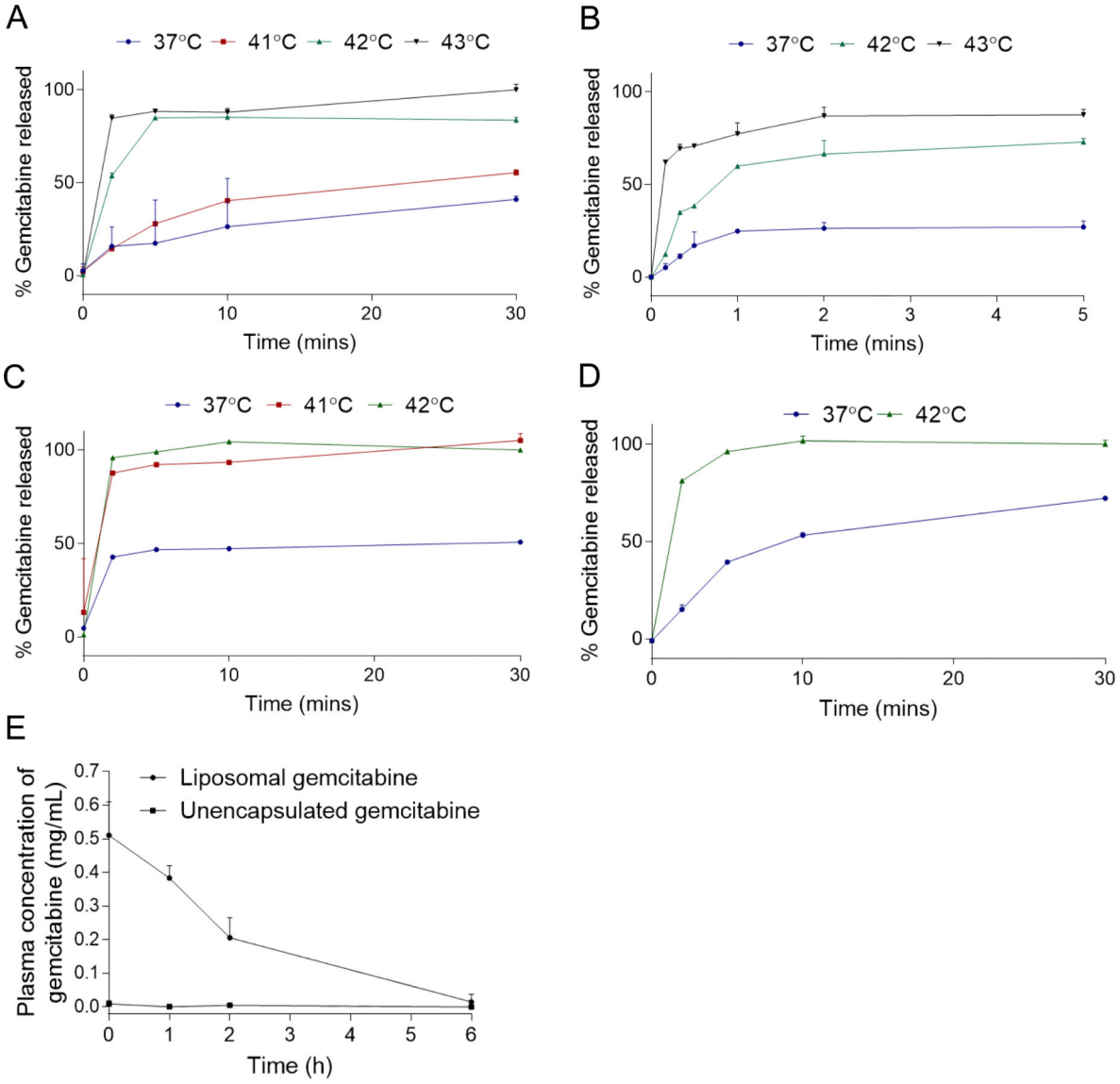

Figure 3. Gemcitabine temperature-sensitive release profiles in serum and *in vivo* pharmacokinetics.

(A-D) DSPC-GemTSLs were incubated in 50% fetal bovine serum at temperatures between 37°C and 43°C and unencapsulated gemcitabine content was measured throughout the 30-minute incubation as a percentage of total gemcitabine released post treatment with Triton X-100. Temperature release profiles of (A-B) DSPC-GemTSLs-10% within a 30-minute (A) and a 5-min (B) time course, (C) DSPC-GemTSLs-12%, and (D) DSPC-GemTSLs-8% without copper. (E) Plasma concentration of gemcitabine either encapsulated in DSPC-GemTSLs-10% (measured after incubation of plasma with Triton X-100) or released from DSPC-GemTSLs-10% after up to 6h of circulation in healthy FVB mice.

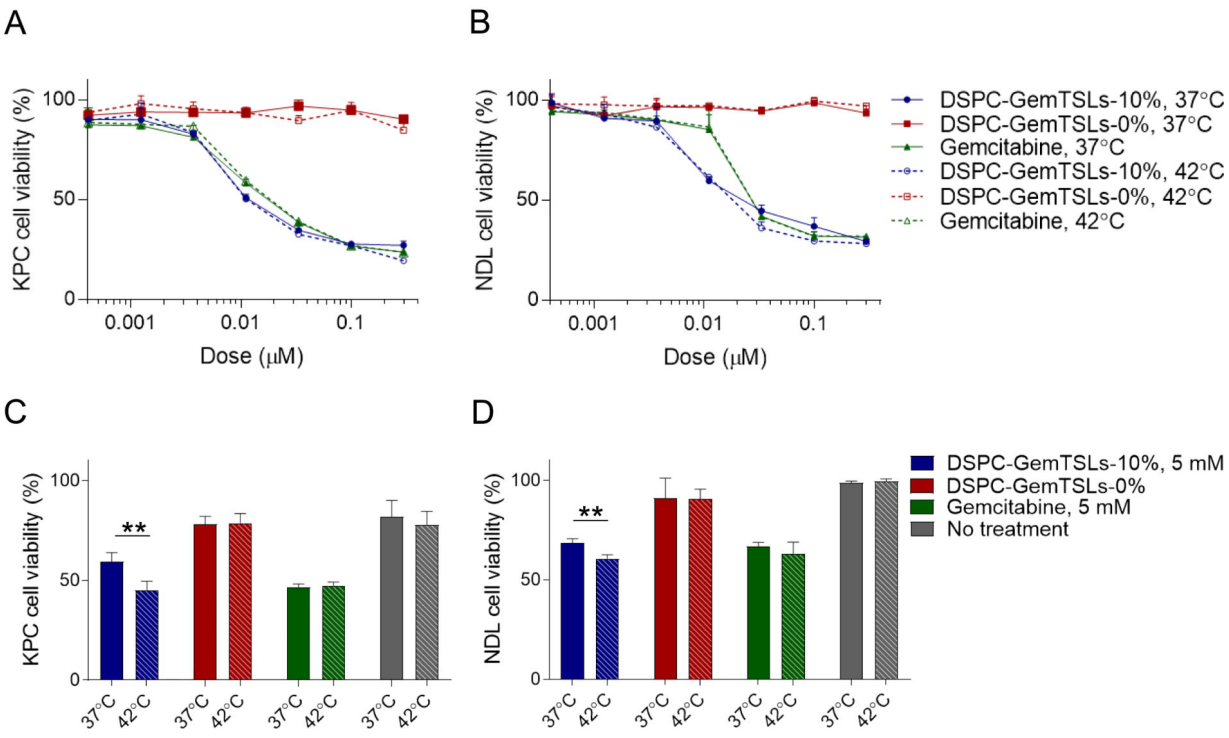

Figure 4. Dose response of KPC and NDL cells to DSPC-GemTSLs-10% with and without temperature-triggered drug release.

Dose response of (A) KPC cells and (B) NDL cells to DSPC-GemTSLs-10%, DSPC-GemTSLs-0%, and free gemcitabine after 20-minute incubation with treatments at 37°C or 42°C, followed by a continuous 48 h incubation at 37°C. Cell viability at 48 h of (C) KPC cells and (D) NDL cells in response to 20-minute incubation with high-dose (5 mM) treatments at 37°C or 42°C, followed by two rinses and incubation in media in the absence of treatments at 37°C for 48 h. Statistical analysis consisted of a Welch's t-test comparing temperature effects within treatment groups. ** $p < 0.01$.

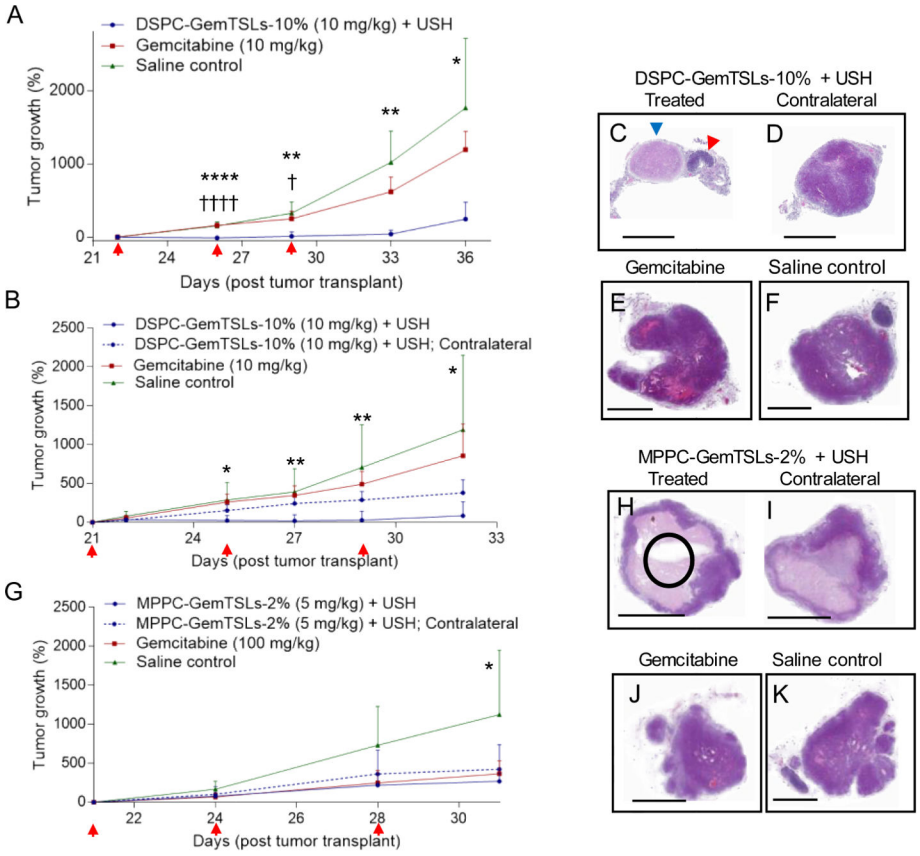

Figure 5. *In* vivo treatment efficacy of GemTSLs with ultrasound hyperthermia (USH) and gemcitabine in NDL tumor-bearing mice after 3 treatments.

Tumor growth is presented as a function of days post tumor transplant, expressed as percent tumor growth for each treatment cohort. Red arrows indicate treatment days. (A) Tumor growth for unilateral NDL tumor-bearing mice intravenously injected with DSPC-GemTSLs-10% (n = 4), gemcitabine (n = 5), or saline (n = 5). (B) Tumor growth for bilateral NDL tumor-bearing mice intravenously injected with DSPC-GemTSLs-10% (n = 5), gemcitabine (n = 4), or saline (n = 4). C-F) H&E staining of (C) DSPC-GemTSLs-10% (10 mg/kg) + USH treated tumor (blue arrow tumor, red arrow lymph node), (D) DSPC-GemTSLs-10% (10 mg/kg) + USH unheated tumor, (E) free gemcitabine (10 mg/kg) treated tumor, and (F) saline control tumor, (G-K) Bilateral NDL tumor-bearing mice were intravenously injected with MPPC-GemTSLs-2% (n = 4), gemcitabine (n = 4), or saline (n = 3). G) Tumor growth post transplant, (H) H&E staining of MPPC-GemTSLs-2% (5 mg/kg) + USH treated tumor (black circle indicates −3 dB US intensity, (I) MPPC-GemTSLs-2% (5 mg/kg) + USH unheated tumor, (J) free gemcitabine (100 mg/kg) treated tumor, and (K) saline control tumor. In mice receiving USH, one tumor in the bilateral tumor models was insonified at 42°C or 41°C for 5 min prior to treatment injection and 30 min following injection of DSPC-GemTSLs-10% or MPPC-GemTSLs-2%, respectively. Scale bar is 3 mm. Statistical analyses consisted of a 1-way ANOVA in (A, B) and 2-way ANOVA in (G) followed by the Tukey Post Hoc test. In (A), * and † denote statistical significances between the average volume of tumors treated with DSPC-GemTSLs-10% and those of saline control tumors or those treated with free gemcitabine, respectively. In (B,G), asterisks denote

statistical significance between the average volume of tumors treated with saline and either DSPC-GemTSLs-10% (B) or MPPC-GemTSLs-2% (G), respectively. In addition, in (B) the average volume of tumors treated with DSPC-GemTSLs-10% was significantly lower than those treated with gemcitabine, $p < 0.05$ on days 25 and 27. * $p < 0.05$; ** $p < 0.01$; **** $p < 0.0001$; † $p < 0.05$; †††† $p < 0.0001$.

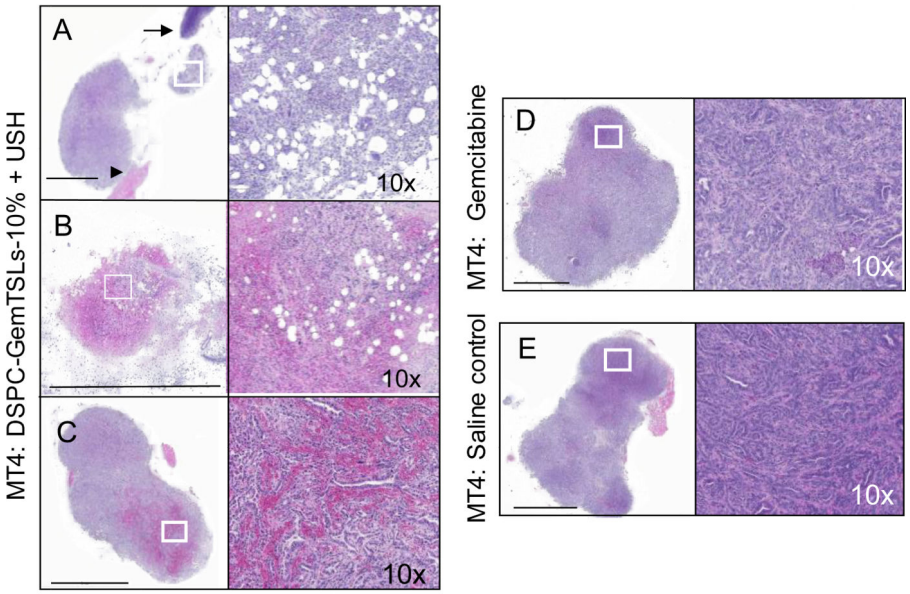

Figure 6. *In* vivo treatment efficacy of DSPC-GemTSLs-10% with ultrasound hyperthermia (USH) and gemcitabine in unilateral mT4 tumor mice after 2 treatments

Mice were intravenously injected with DSPC-GemTSLs-10% (n = 4), gemcitabine (n = 5), or saline (n = 6). In mice receiving USH, the tumor was insonified at 42°C for 5 min prior to treatment injection and 30 min following injection. H&E staining of (A-C) DSPC-GemTSLs-10% (10 mg/kg) + USH treated tumors (left panels and 10x magnification, right panels), (D) free gemcitabine (10 mg/kg) treated tumor (left panel and 10x magnification, right panel), and (E) saline control tumor (left panel and 10x magnification, right panel). In (A), the arrow and the arrowhead point to lymph node and muscle tissue, respectively. Scale bar is 3 mm.

Table 1:

Summary of lipid formulations evaluated

Formulation name	Temperature sensitive core lipid	Stabilizing or rapid release lipid	PEGylated lipid	Molar ratio
Lyso-PPC-GemTSLs	1,2-dipalmitoyl-sn-glycero-3-phosphocholine	1-palmitoyl-2-hydroxy-*sn*-glycero-3-phosphocholine	1,2-distearoyl-sn-glycero-3-phosphoethanolamine-N-methoxy polyetheneglycol-2000	86:10:4
Lyso-SPC-GemTSLs		1-stearoyl-2-hydroxy-*sn*-glycero-3-phosphocholine		86:10:4
DSPC-GemTSLs		1,2-disteraroyl-sn-glycero-3-phosphocholine		80:15:5
MPPC-GemTSLs		1-myristoyl-2-palmitoyl-*sn*-glycero-3-phosphocholine		89:7:4
MSPC-GemTSLs		1-myristoyl-2-stearoyl-*sn*-glycero-3-phosphocholine		89:7:4